A MICROWAVE STUDY OF CORONAL EJECTA

M. R. Kundu[1], A. Nindos[1], J.-P. Raulin[2], K. Shibasaki[3], S. M. White[1], N. Nitta[4], K. Shibata[5] and M. Shimojo[5]

[1] Astronomy Department, University of Maryland, MD 20742

[2] CRAAE (Mackenzie, INPE, USP, UNICAMP) Instituto Presbiteriano Mackenzie, Rua da Consolacão 896, 01302-000 São Paulo, SP, Brazil

[3] Nobeyama Radio Observatory, Minamimaki, Minamisaku, Nagano 384-13, Japan

[4] Lockheed Martin Solar and Astrophysics Laboratory, O/H1-12, B/252, 3251 Hanover Str., Palo Alto, CA 94304

[5] National Astronomical Observatory, Mitaka, Tokyo, 181-8588, Japan

ABSTRACT

Using Nobeyama 17 GHz data, we have studied the radio properties of 19 coronal jets identified in Yohkoh SXT X-ray observations. The radio data provide information on the physical conditions in the jets which complements the data from the X-ray surveys. Microwave emission was associated with the majority of the X-ray jets in our sample. The radio emission typically came from the base or the base and lower part of the jets. We detected radio emission from almost all jets which showed flare-like activity at their bases. The jets which were not associated with radio emission did not show any significant increase in X-ray emission at their bases. The strongest radio emission came from two of the largest jets in our sample. Our data show a general correlation between the X-ray jet fluxes and the associated radio fluxes. The 17 GHz time profiles were gradual and unpolarized, implying that the emission was thermal. In a two-sided-loop jet (July 22, 1992 event) and one anemone-type jet (February 9, 1993 event), the observed microwave fluxes from the lower part of the jets were well above the fluxes calculated from the computed physical parameters of the soft X-ray-emitting material on the basis of thermal free-free emission. We interpret the large discrepancies in terms of the presence of lower temperature material which cannot be detected by the SXT (the SXT is most sensitive to hot plasma above 2×10^6 K) but which produces strong microwave free-free emission. This is the first time that such material has been observed in two-sided-loop type jets. We also observed motion of a jet-associated microwave source with a velocity of 55 km/sec. The microwave motion occurred after the appearance of the X-ray jet. There is clear evidence that the microwave emission of that source was associated with the jet and not with the associated small flare.

Subject headings: Sun: activity – Sun: corona – Sun: radio radiation – Sun: X-rays, gamma rays

1. Introduction

The high spatial and temporal resolution of the soft X-ray imaging telescope (SXT) on board the Yohkoh satellite (Tsuneta et al. 1991) allows the detection of X-ray jets which are transitory enhancements with well-collimated motion (Shibata et al. 1992). The jet phenomenon involves the ejection of 10^{12} - 10^{14} g of coronal material with apparent velocities between 10 and 400 km/s (Shibata, Yokoyama, & Shimojo 1994). Shimojo et al. (1996) performed a statistical analysis of 100 jets and found that most of them were associated with small flares (subflares or microflares) which occurred in complexes of X-ray bright points, emerging flux regions or active regions. Their lengths range from 10^4 km to 4×10^5 km, and their lifetimes range from a few minutes to several hours.

Shibata, Nozawa, & Matsumoto (1992) proposed that the jet plasma is accelerated and heated by magnetic reconnection between emerging flux and the pre-existing magnetic field. Two types of such interaction have been observed (Shibata, Yokoyama, & Shimojo 1994; Shibata 1998). Most frequent is the anemone type which exhibits vertical or oblique jets that usually occur when emerging flux appears in coronal holes. The other is the two-sided-loop type which occurs when emerging flux appears in a quiet region where the magnetic field is almost horizontal. In the latter case hot plasma is ejected along coronal loops away from both sides of the emerging flux. Yokoyama and Shibata (1996) performed MHD simulations of X-ray jets based on the magnetic reconnection model. They reproduced successfully the two observed types of jets and their general features.

Kundu et al. (1995) and Raulin et al. (1996) reported the detection of nonthermal radio emission in the form of metric type III bursts from X-ray bright point/anemone type X-ray jets. The type III emission shows that particle acceleration is taking place in jets as is normal in ordinary flares. No type III bursts have been detected in association with two-sided-loop type jets because the magnetic field is parallel to the photosphere and type III emitting electrons propagate along open field lines (Kundu et al. 1998). Kundu, Shibasaki and Nitta (1997) reported the first detection of microwave emission from X-ray jets using the Nobeyama Radioheliograph at 17 GHz. The 17 GHz emission was unpolarized and came mainly from the base of the jets although in one case, emission originated from the lower part of the jet as well. Thus in most cases, the jet itself must be optically thin at 17 GHz.

In this paper, we extend the previous study of individual jets by Kundu, Shibasaki and Nitta (1997) . We study a large sample of X-ray jets observed by SXT and we compute the physical properties of the ejected plasma when possible. We then compare the SXT information with images of the jets obtained with the Nobeyama Radioheliograph at 17 GHz. The basic features of the jet-associated radio emission are presented. Note that SXT is most sensitive to hot plasma above 2×10^6 K, whereas the microwave observations can be sensitive to cooler material as well. Thus, in principle, the radio images of the jets could provide information on the physical conditions of the jets that is not available from the SXT images.

2. Observations and data reduction

The methodology of our study was to make 17 GHz images for periods during which the Yohkoh SXT observed X-ray jets. We used 19 different jet events which took place from July 1992 to March 1995. The X-ray observations that we used were taken either in the partial frame mode (images made with the thin Aluminium, Al 1265 Å, filter or thick Al 11.6μm filter, with field of view $5' \times 5'$, pixel size $2.46''$ and time resolution 32 s) or in the full-frame mode (images made with the thin Al filter or the "sandwich" Al/Mg/Mn filter with full-disk field of view, pixel size $4.91''$ and time resolution of about 2 min or more). The full-frame images were used only in cases when jets were not recorded in the partial frame images. These events are denoted with an asterisk in Table 1. The filters we used are sensitive to soft X-ray emission between 3 and 40 Å, which is produced by plasma with temperatures from 1.5×10^6 K to a few 10^7 K (Tsuneta et al. 1991). We used the thin Al filter to identify the jets visually because it is more sensitive to faint brightenings. The SXT images were processed with the standard calibration software, which does the data decompression, background subtraction, correction for solar rotation and normalization of the images to compensate for exposure differences. Using the filter ratio technique (Hara et al. 1992), we calculated the electron temperatures and emission measures of the jets. In weak events, we averaged signals from several pixels in order to improve the signal-to-noise ratio. We converted emission measure to density, assuming the filling factor to be unity and a range of thickness at each location comparable with the apparent width of the jet.

Since the jets undergo rapid changes, the evaluation of the plasma parameters derived by the filter ratio method for the full-frame-images (FFIs) must be done very carefully (Shimojo et al. 1998). In our analysis, we rejected the successive FFIs observed with the two filters more than 2 min apart from one another. For the rest of the FFIs, we computed the plasma parameters for the time of each Al (sandwich)-filter image using both the previous and following sandwich (Al) images. In all cases, the uncertainties due to the time variability of the jets were larger than the uncertainties introduced by photon statistics. For the cases in which the two pairs of the computed plasma parameters at a given time, agreed to within a factor of 2, we re-calculated rough values of the emission measures using the X-ray intensities of the jets and assuming temperatures between 3×10^6 K and 7×10^6 K (e.g. Shibata et al. 1994; Kundu, Shibasaki, & Nitta 1997). In our subsequent analysis, we used the values derived by the filter-ratio method only in the cases in which the calculated emission measures by the two methods overlapped.

The Nobeyama Radioheliograph (NRH) observations at 17 GHz were made with a spatial resolution of $10''$ and a temporal resolution of 0.5-1 min. The NRH records both right-handed and left-handed circular polarization and its field of view covers the entire Sun. It has a dynamic range better than 25 db (Koshiishi et al. 1996). The development of new software (Koshiishi 1996) permits much higher dynamic range which is necessary for the analysis of low brightness solar phenomena. Using this new software, we produced full disk maps at 17 GHz corresponding to the times of the soft X-ray jets of our collection. We should point out that the NRH full-disk images are ideally suited for the study of jet-like phenomena which can occur both in and well away from active regions of the Sun.

3. Results

3.1. General properties of jet-associated radio emission

In Table 1 we present the X-ray jets that we studied. Our sample contained one two-sided loop type jet (the one which was observed on July 22, 1992). All the others were either vertical or oblique jets. Most of the jets (14 out of 19) were associated with small flare-like events at their bases (see also Shimojo et al. 1996). None of these events triggered the flare mode of the SXT; the range of their SXT peak intensity was 8×10^2–10^6 DN/sec while the corresponding value of the SXT active region transient brightenings studied by Shimizu (1995) was 10^3-10^6 DN/sec.

Table 1 indicates that microwave emission was observed in the vast majority of the X-ray jets (about 80%, see also Kundu 1998; Kundu, Shibasaki, & Nitta 1997). The radio emission was associated either with the closed loops where the collimated X-ray-emitting plasma flow emanated (hereafter referred to as “base of the jet”) or with the base and the lower part of the collimated plasma flows (hereafter referred to as “lower part of the jets”). For quantitative analysis of the jets, we measured the fluxes in the available sequences of radio images by intergrating over the smallest region of each image which contained the X-ray jet. The peak radio flux of each jet is given in Table 1. We also estimated the rms noise σ of the radio maps by subtracting two successive maps and summing over a region of similar size in the portion of the difference image corresponding to the bright extended active region emission.

In the events where microwave emission was detected, the parts of the jets emitting

17 GHz emission must have higher optical depth than the non-microwave-emitting parts of the jets. This implies that in all cases, the upper parts of the jets were optically thin. We should point out that microwave emission was detected at the base of 13 out of 14 jets in which X-ray intensity increased at their bases. Three of the four jets that were not associated with radio emission did not show any X-ray flare-like activity at their bases. All the jets with no detectable microwave emission were small events with apparent projected lengths between 1.75×10^4 and 4.8×10^4 km. Such short jet lengths lie at the low end of the length distribution of a large sample of jets analyzed by Shimojo et al. (1996) . However, even in these cases, the jet plasma might have emitted 17 GHz emission which was below the NRH detection threshold (i.e. the 3σ level of the radio maps). The same argument also applies to the absence of radio emission from the upper part of all X-ray jets of our sample.

In Figure 1, we present a scatter plot of the maximum radio jet fluxes versus maximum X-ray fluxes. For the X-ray flux computations both bases and collimated parts of the jets were considered. At 17 GHz, we could distinguish between the base emission and emission from the lower part of the jet only for July 22, 1992 and February 9, 1993 events. For these events, the radio emission from the lower part of the jet was plotted while for the other events, the total radio jet flux was used. At both wavelengths the fluxes were computed after the pre-event fluxes had been subtracted out. The strongest radio emission corresponds to the two-sided-loop type jet of July 22, 1992 (see section 3.3) and the anemone-type jet (see section 3.2) which was observed on February 9, 1993. Both of them were among the largest of our sample. On the other hand, the 17 GHz flux of the strongest X-ray jet (the "Dec 22d 93" entry of Table 1) was only 0.09 SFU; that jet occurred almost at sunset in Japan and the microwave sources were elongated due to the elongated shape of the beam. The correlation coefficient of the X-ray and radio fluxes was 0.42. If we do not take into account the "Dec 22d 93" event, we get a correlation coefficient of 0.73, which implies moderate to good correlation between the X-ray and the radio fluxes. The fact that we did not find a better correlation coefficient might imply that in some jet events the X-ray and microwave emission come from different loops (as suggested by Kundu, Shibasaki, & Nitta 1997) but it might also be a consequence of the inadequate spatial resolution and/or sensitivity of the NRH observations. It may also be associated with the large uncertainties involved in the calculation of the X-ray and radio fluxes. Some scatter is also expected in the correlation if SXT did not observe the peak of some jet events, especially when only full-frame images were available (the highest cadence of the SXT in full-frame mode is 2 min and is more typically 4 min whereas the cadence of the 17 GHz data is 1 min or better).

The light curves of the 17 GHz jet emission were gradual in most cases. Only the April 21a, 1993 and January 6 1994 events showed somewhat faster rise and decay (about 1.5-2 min) but the duration of their brightness peaks was rather broad, about 5 min. In all events, the radio emission was unpolarized. These features suggest that the 17 GHz emission was thermal. In a typical impulsive flare we would expect the nonthermal emission at 17 GHz to be stronger than any thermal free-free component. Of course, we cannot exclude the possibility that nonthermal emission was present but relatively weak, due either to a low turnover frequency in the radio spectrum or to a particularly steep radio spectrum at high frequencies (see also White et al. 1995). The general properties of the radio emission from the X-ray jets are consistent with the properties of the two events which were discussed by Kundu, Shibasaki and Nitta, (1997) .

The computed electron temperatures and emission measures of the jets (see discussion in section 2) were used to calculate the 17 GHz flux from the observed soft X-ray-emitting material on the basis of thermal free-free emission (see e.g. Pohjolainen et al. 1997 for the formula). For the events which showed X-ray base enhancement and radio emission from the base of the jet only, the computed radio flux associated with the jet base can be compared directly to the observed radio flux from the jet base. Using the criteria defined in section 2, we computed reliable plasma parameters for three such events (the Apr 21b, 93, Oct 03, 93 and Mar 31, 95 entries of Table 1). The computed fluxes were in agreement with the observed fluxes, within a factor of 1.3, which is reasonable given the uncertainties involved. The remaining 3 events of this class were small jets, associated with X-ray bright points which were recorded in full-frame images only.

In two cases, the computed radio fluxes associated with the lower parts of the jets were well below the observed radio fluxes. These events will be presented in the two following sections.

3.2. The February 9, 1993 jet

This is a spectacular anemone-type jet which occurred about 220″ east of active region NOAA 7417. No partial-frame SXT images were available. The exposure time of the first SXT frame was only 78 ms but it shows some weak loop-like X-ray emission (near the center of the upper left frame of Figure 2). The associated microwave emission is very low. At 03:59 UT the X-ray emission from that region increased considerably and there is evidence of plasma ejection from its northeast edge but the radio emission is still insignificant. At 04:07 UT the X-ray emission from the base of the jet as well as the emission of the collimated jet itself increased further. In addition, the collimated ejected material of the jet appears to have enhanced brightness at its eastern and western edges. At the same time the microwave emission consists of two components: one is associated with the base of the jet (source 1 in Figure 2) and the other with the lower east part of the jet (source 2 in Figure

2). There is no radio emission associated with the west part of the jet. The last available SXT image shows that the collimated plasma emission has decayed but the base emission is still strong. The X-ray light curves (Figure 3) also show the delay between the decay of the base emission with respect to the decay of the collimated jet emission. The corresponding radio light curves indicate that 17 GHz emission reaches maximum values in the final stages of the X-ray jet.

Only the electron temperatures and emission measures computed for the 04:07 UT frame satisfied the criteria that we defined in section 2. In Table 2 we give the electron temperatures and emission measures that were computed by the filter ratio method for the two pairs of images which contained the 04:07 UT frame together with the computed free-free radio fluxes and the observed radio fluxes. If we use the average X-ray intensity of the jet and assume temperatures between 3×10^6 K and 7×10^6 K, we obtain values for the emission measures consistent with the filter-ratio results. If the thickness of the jet is equal to its apparent width, we get a density of $1.1 \pm 0.6 \times 10^9$ cm^{-3}. The 17 GHz computed and observed fluxes for the base of the jet are consistent, given the large uncertainties involved. However, the predicted radio flux for the east part of the jet is 10-22 times lower than the observed flux. We may interpret this disagreement in terms of the presence of a lower temperature material which cannot be seen by the SXT but which produces significant microwave free-free emission. The predicted flux for the west part of the jet at 04:07 UT is below the NRH detection limit (the 3σ level of the radio maps is 0.03-0.06 SFU). It seems that the additional cooler material was present only at the eastern part of the jet at least since 04:07 UT. If we attribute the entire microwave flux to cooler material not detectable by SXT then the flux of the cool jet reaches a maximum value about 10 min after the X-ray maximum.

3.3. The July 22, 1992 jet

A preliminary discussion of this jet was given by Kundu (1998) . It was the only two-sided-loop type jet of our sample. Unfortunately, no PFIs for this event were available. The jet occurred about $270''$ northeast of the small sunspot of active region NOAA 7235, in a region where relatively weak loop emission was observed by SXT. The first SXT image was obtained at 01:16 UT (upper left frame of Figure 4) and clearly shows enhanced X-ray emission at the north-east part of the loop configuration. The flux of the X-ray enhancement was about 8.5×10^4 DN/sec which is of the order of fluxes of active region transient brightenings reported by Shimizu (1995) . According to NRH data, the region started to flare up after 01:09 UT (Figure 5, dot-dashed line); the microwave emission showed a rather gradual rise for about 5 min. The next SXT frame was obtained at 01:53 UT and shows the two-sided-loop type jet: it seems that the region flared up due to the emergence of new flux and subsequently hot plasma was ejected along coronal loops away from both sides of the emerging flux. The last SXT image of the jet obtained at 02:02 UT but appears to be similar to the 01:53 UT image. When the SXT observations resumed at 02:55 UT, no trace of the jet was found. Figure 5 shows that the microwave component (source C) associated with the emerging flux exhibited a very slow decay after it reached maximum flux of 0.38 SFU. The NRH images clearly show the microwave counterparts to the ejected hot X-ray-emitting material (the sources A and B in Figure 4). The 17 GHz light curves of these sources indicate that the ejection of material started after 01:34 UT. The flux of these sources was rising while that of component C decayed.

Only the electron temperatures and emission measures computed for the two pairs of images which contained the 01:53 UT frame satisfied the criteria that we defined in section 2. The values derived by the filter ratio method are given in Table 3 along with the computed and observed radio flux at 01:53 UT. We list the parameters for the emerging flux component as well as the two components associated with the plasma ejection. Using the average X-ray intensity of the jet and assuming temperatures between 3×10^6 K and 7×10^6 K, we obtained values for the emission measures consistent with the filter-ratio results. If the thickness of both sides of the jet was $15''$ then the computed jet densities would be $0.97 \pm 0.45 \times 10^9$ cm^{-3}. Our computed temperatures and densities are in agreement with the study of Shimojo et al. (1998) . The computed 17 GHz emission for the emerging flux area (source C) is in agreement with the observed microwave flux. However, the computed radio fluxes for both sides of the jet (sources A, B) are 18-40 times lower than the corresponding observed fluxes. These large discrepancies may be due to a lower temperature plasma which emits microwaves but cannot be detected by the SXT. Unfortunately, no Hα data were available, so we cannot determine directly whether the additional cooler material was chromospheric or originated from the chromosphere-corona transition region. We should note that the simulations of the two-sided-loop type jets by Yokoyama and Shibata (1996) predict the existence of cool dense chromospheric plasma which is ejected from a current sheet along with the hot plasma which is the X-ray jet. Wilhelm et al. (1998) also reported plasma ejections observed in EUV emission lines by SUMER on board SoHO. The ejection occurred within a network cell close to a coronal hole and the deduced geometry of the event was similar to the two-sided-loop type jet geometry.

An inspection of Fig. 4 (middle and right frames of bottom row) clearly shows that the microwave source A expands. Using the full set of the 1-min-cadence NRH images, we found that the apparent velocity of expansion of radio source A (western jet) was about 55 km/s. We note that the motion of the microwave-emitting material occurred after the appearance of the two-sided-loop X-ray jet. Unfortunately, the number and cadence of the full-frame SXT images was not adequate to derive reliable information about the velocity of the X-ray-emitting material. The corresponding SXT images, however, did not show any significant changes. The reason that Kundu, Shibasaki & Nitta (1997) did not find any motions of jet-associated 17 GHz sources may be that the dataset they studied was rather limited: they studied three events and only one of them showed microwave emission at the lower part of the jet. The velocity we measured is close to the lower end of the observed velocities of Hα surges (40-100 km/s, see Zirin 1988). The observed motion of microwave source A verifies that the microwave emission of that source was associated with the jet and not with the small flare. The same was true for the February 9, 1993 event where we distinguished the microwave emission due to the X-ray jet from microwave emission due to small flare at the jet base. These two cases argue strongly for a real association of microwave emission with X-ray jets.

4. Conclusions

In this paper, we studied the microwave emission of coronal plasma ejections. We used a sample of 19 X-ray jets and compared the X-ray jet emission with the 17 GHz emission from the regions where the jets occurred. Microwave emission was detected from the vast majority (about 80%) of the X-ray jets. The radio emission was associated either with the base of the jets or with the base and the lower part of the jets. We detected radio emission from all but one of the jets which showed flare-like activity at their bases. Moreover, we detected no significant increase of X-ray emission from the base of three of the four jets that were not associated with radio emission. However, we cannot exclude the possibility that even some of these jets emitted weak microwave emission which was below the detection threshold of the NRH. The strongest radio emission was associated with two of the largest jets of our sample. The correlation coeffficient between the maximum X-ray jet fluxes and the associated radio fluxes is 0.73. Thus our data show a general correlation between the X-ray and radio fluxes. The lack of a better correlation might imply that in some cases the X-ray and the microwave emission come from different loops but it may also be associated with the large uncertainties involved in the calculation of the radio and X-ray fluxes. It is also possible that the SXT did not observe the peak of some jet events, especially when only full-frame images were available. The light curves of microwave jet emission were gradual and unpolarized implying that the emission was thermal. The general properties of the microwave emission associated with the X-ray jets are consistent with the results presented by Kundu, Shibasaki and Nitta (1997) .

When possible, we computed the electron temperatures and emission measures of the X-ray-emitting jet plasma. Our computations are in general agreement with the results derived from another data set by Shimojo et al. (1998) . We used the computed X-ray plasma parameters to derive the 17 GHz fluxes on the basis of thermal free-free mechanism. For the events which showed enhancement of the X-ray jet base emission and radio emission from the base of the jet only, the computed radio fluxes associated with the jet bases are in agreement with the observed ones. This result suggests that the emission mechanism of the brightenings associated with the bases of the jets at 17 GHz is thermal free-free.

We found two events in which the computed free-free fluxes were well below the observed radio fluxes. One event (July 22, 1992) was a two-sided-loop type jet and the other (February 9, 1993) was an anemone-type jet. Both events were among the largest of our sample. Since SXT is sensitive only to hot plasmas above 1.5×10^6 K, we interpreted the large discrepancies in terms of lower temperature plasmas which cannot be detected by SXT but are sensitive to microwave free-free emission. In both cases the lower temperature material was associated with the lower part of the jets. The number of cases where the observed 17 GHz flux was well above the flux computed from the SXT plasma parameters (2 out of 19) should be considered as a lower limit. Some of the other jets may emit weak microwave emission which comes from a lower temperature plasma but it is below the detection threshold of NRH.

The absence of Hα data for these two events does not give us any direct clues whether the origin of lower temperature material was chromospheric or originated from higher layers of the solar atmosphere. At 17 GHz, the maximum brightness temperatures of the two jets that we presented was about 2×10^4 K. If we assume that the brightness temperature of the quiet Sun at 17 GHz is 10^4 K then we need an optical depth of about 0.1 to get a contribution of 10^4 K from a plasma at a temperature of 10^5 K. In an isothermal free-free model this leads to average densities of about 0.9×10^9 cm^{-3} for the two jets. This value is lower than is typical of 10^5 K plasmas. On the other hand, if the electron temperature is 10^6 K, the required optical depth is 0.01. This leads to a density of 1.6×10^9 cm^{-3}. If we take into account the uncertainties, the densities derived from the SXT plasma parameters for the two jets were between $0.5 - 1.7 \times 10^9$ cm^{-3} (sections 3.2 and 3.3). The large uncertainties involved in these computations do not allow us to derive reliable constraints on the temparature of the material which cannot be seen by the SXT.

The simulations by Yokoyama & Shibata (1996) predict the existence of cool jets which are adjacent to hot coronal jets for the anemone-type jets as well as for the two-sided loop type jets. The temperature distribution in their simulations is complex and there is always a $T_e \sim 10^5$ K plasma between their cool (chromospheric) and hot (coronal) jets. Our observations provide the first direct confirmation for the existence of lower temperature material in the two-sided-loop type jets which cannot be detected by the SXT.

We observed, for the first time directly, the motion of a jet-associated microwave source. The source associated with the western side of the two-sided-loop jet expanded with a velocity of 55 km/s. This velocity is consistent with typical observed velocities of Hα surges. For comparison, we note that the apparent velocities of X-ray jets range from 10 km/s to 400 km/s. But the statistical study of 100 jets by Shimojo et al. (1996) showed that their average value of velocities is 200 km/s. The motion of the microwave-emitting material occurred after the appearance of the two-sided-loop X-ray jet when the corresponding SXT images did not show any significant changes. For the February 9, 1993 event, the radio jet was also delayed with respect to the X-ray jet. The cool jet reached a maximum value 10 min after the X-ray jet maximum. Schmieder, Golub and Antiochos (1994) reported a case where the chromospheric Hα plasma was delayed by 3-4 min with respect to an X-ray brightening. Delays of X-ray emission with respect to Hα surges have also been observed (e.g. Canfield et al. 1996). In both cases that we presented, our data cannot answer unambiguously the question of whether this cooler material is due to the same ejection mechanism as the hot jet or whether it is the result of cooling of the jet. The delay of the microwave emission with respect to the X-ray emission in the February 9, 1993 event could be a signature of the cooling of the X-ray jet. However, since cooled material generally falls back into the chromosphere, the expansion of the source A of the July 22, 1992 event clearly contradicts such an interpretation.

Because most jets are associated with small flares at their bases and a significant amount of the jet-associated microwave emission originates from the base, there is always the issue of whether the microwave emission is associated with the flare or the jet. However, in some cases we can clearly distinguish the microwave emission due to the X-ray jet from microwave emission due to flare at the jet base. The February 9, 1993 event provides such an example. Another example is the August 25, 1992 jet which was presented by Kundu, Shibasaki, & Nitta (1997) . Furthermore, the motion of a microwave component associated with the two-sided-loop type jet that we observed confirms that the microwave emission of that source was associated with the jet and not with the small flare. The two cases which were presented in detail in this paper show that microwave observations can serve as a powerful plasma diagnostic and can provide information complementary to the more common X-ray surveys of plasma ejections.

5. ACKNOWLEDGMENTS

This research at the University of Maryland was carried out with support from NSF grants ATM 96-12738 and INT 97 22489 and by NASA grant NAG 5-6257.

REFERENCES

Canfield, R. C., Reardon, K. P., Leka, K. D., Shibata, K., Yokoyama, T., & Shimojo, M. 1996, ApJ, 464, 1016.

Hara, H., Tsuneta, S., Lemen, J. R., Acton, L. W., & McTiernan, J. M. 1992, PASJ, 44, L135.

Koshiishi, H. 1996, Ph.D. Thesis, University of Tokyo.

Koshiishi, H., et al. 1996, PASJ, 46, L33.

Kundu, M. R. 1998 in “Solar Jets and Coronal Plumes”, ed. T.-D. Guyenne (ESA SP 421; Noordwijk:ESA), 179.

Kundu, M. R., Shibasaki, K., & Nitta, N. 1997, ApJ, 491, L121.

Kundu, M. R., Raulin, J.-P., Nitta, N., Hudson, H. S., Shimojo, M., Shibata, K., Raoult, A. 1995, ApJ, 447, L135.

Kundu, M. R., Raulin, J.-P., Nitta, N., Shibata, K., & Shimojo, M. 1998, Sol. Phys., 178, 173.

Pohjolainen, S., Valtaoja, E., Urpo, S., Aurass, H. 1997, Sol. Phys., 173, 131.

Raulin, J.-P., Kundu, M. R., Hudson, H. S., Nitta, N., & Raoult A. 1996, A&A, 306, 299.

Shibata, K. 1998 in “Solar Jets and Coronal Plumes”, ed. T.-D. Guyenne (ESA SP 421; Noordwijk:ESA), 137.

Shibata, K., Nozawa, S., & Matsumoto, R. 1992, PASJ, 44, 265.

Shibata, K., Yokoyama, T., Shimojo 1994, in Proc. of Kofu Symposium, “New Look at the Sun with Emphasis on Advanced Observations of Coronal Dynamics and Flares”, ed. S. Enome, T. Hirayama , 75.

Shibata, K., et al. 1992, PASJ, 44, L173.

Shibata, K., Nitta, N., Strong, K. T., Matsumoto, R., Yokoyama, T., Hirayama, T., Hudson, H., & Ogawara, Y. 1994, ApJ, 431, L51.

Shimizu, T. 1995, PASJ, 47, 251.

Shimojo, M., Hashimoto, S., Shibata, K., Hirayama, T., Hudson, H. S., Acton, L. W. 1996, PASJ, 48, 123.

Shimojo, M., Shibata, K., Hori, K., Yokoyama, T. 1998 in "Solar Jets and Coronal Plumes", ed. T.-D. Guyenne (ESA SP 421; Noordwijk:ESA), 163.

Schmieder, B., Golub, L., Antiochos, S. K. 1994, ApJ, 425, 326.

Tsuneta, S., Acton, L., Bruner, M., Lemen, J., Brown, W., Caravalho, R., Catura, R., Freeland, S., Jurcevich, B., Morrison, M., Ogawara, Y., Hirayama, T., & Owens, J. 1991, Sol. Phys., 136, 37.

White, S. M., Kundu, M. R., Shimizu, T., Shibasaki, K., & Enome, S. 1995, ApJ, 450, 435.

Wilhelm, K., Innes, E. E., Curdt, W., Kliem, B., Brekke, P., 1998 in "Solar Jets and Coronal Plumes", ed. T.-D. Guyenne (ESA SP 421; Noordwijk:ESA), 103.

Yokoyama, T., & Shibata, K. 1996, PASJ, 48, 353.

Zirin, H. 1988, "Astrophysics of the Sun", Cambridge University Press, Cambridge.

This preprint was prepared with the AAS LaTeX macros v4.0.

FIGURE CAPTIONS

Fig. 1.— Scatter plot between the maximum flux of the X-ray jets and the corresponding maximum microwave flux. Both the bases and the collimated parts of the X-ray jets were taken into account in our calculations. At 17 GHz, we could distinguish between the base emission and the emission of the lower part of the jet only in the cases of the July 22, 1992 and the February 9, 1993 events. For the other events, the total radio flux was used. The July 22, 1992 jet was a two-sided-loop type jet and we used the average values of the maximum X-ray and microwave fluxes from the two sides.

Fig. 2.— The February 9, 1993 anemone-type jet. Top row: SXT images of the jet extracted from full-frame images of the Sun (negative display). Bottom row: the corresponding NRH 17 GHz emission (negative display). All SXT images presented in this paper have been obtain with the thin Aluminium filter. In this and subsequent solar images the axes labels indicate seconds of arc from the center of the disk. Solar north is up and solar east to the left. The boxes indicate the regions we used for the computation of the X-ray flux from the base of the jet and the eastern side of the jet.

Fig. 3.— Time profiles of the X-ray emission and microwave emission in total intensity, I, from the February 9, 1993 jet. The solid lines indicate the 17 GHz light curves and the dashed lines indicate the X-ray light curves. Top frame: the east part of the collimated plasma ejection. Bottom frame: the base of the jet.

Fig. 4.— Same as in Fig. 2 for the July 22, 1992 two-sided-loop type jet. The boxes indicate the regions we used for the computation of the X-ray flux from sources A and B.

Fig. 5.— Time profiles of the microwave emission in total intensity, I, of the sources associated with the July 22, 1992 jet. The solid line indicates the time profile of the east source (source B) and the dashed line indicates the time profile of the west source (source A) of the two-sided-loop type jet. The dash-dotted line shows the light curve of the source associated with the initial emergence of new flux (source C).

Table 1. X-ray jets and 17 GHz radio emission

Date	SXT Start (UT)	SXT End (UT)	SXT base enhanc.	17 GHz emission	Radio flux SFU	RMS noise (SFU)
*Jul 22, 92	01:16	$> 02:15$	Yes	Base/both sides	0.18/0.22	0.017
Aug 17, 92	01:28	$> 02:04$	No	Base	0.09	0.011
*Feb 09, 93	03:59	$> 04:16$	Yes	Base/lower part	0.35/0.20	0.017
Apr 21a, 93	01:10	$> 01:28$	No	Base/lower part	0.11	0.019
*Apr 21b, 93	01:10	$> 01:36$	Yes	Base	0.15	0.020
Jul 12, 93	03:11	03:11	No	No	...	0.016
*Sep 24, 93	04:56	04:58	Yes	Base	0.08	0.021
Oct 02, 93	04:10	04:17	Yes	No	...	0.014
Oct 03, 93	03:04	$> 03:34$	Yes	Base	0.12	0.011
*Jan 05a, 94	03:03	03:12	Yes	Base	0.09	0.018
Jan 05, 94	03:01	03:28	No	No	...	0.019
*Jan 06, 94	02:00	$> 02:02$	Yes	Base	0.065	0.017
Jul 13, 94	00:57	01:04	No	No	...	0.012
Dec 22a, 94	01:58	02:02	Yes	Base/lower part	0.11	0.013
Dec 22b, 94	02:27	$> 02:29$	Yes	Base/lower part	0.15	0.015
Dec 22c, 94	03:31	03:48	Yes	Base/lower part	0.08	0.013
Dec 22d, 94	05:25	05:43	Yes	Base/lower part	0.09	0.016
Dec 26, 94	01:38	02:08	Yes	Base/lower part	0.13	0.017
Mar 31, 95	05:55	06:18	Yes	Base	0.09	0.009

Note. — * denotes the SXT jets which were observed in partial-frame images.

Table 2. Data for the February 9, 1993 jet

Component	Time UT	T_{SXT} ($\times 10^6$ K)	EM_{SXT} ($\times 10^{45}$ cm^{-3})	17 GHz Flux (predicted; SFU)	17 GHz Flux (Observed; SFU)
Jet base	04:07	4.65 ± 1.05	245 ± 65	0.25 ± 0.09	0.27
East jet	04:07	5.9 ± 1.1	13.65 ± 4.35	0.013 ± 0.005	0.18
West jet	04:07	6 ± 0.8	12.45 ± 3.55	0.011 ± 0.004	...

Table 3. Data for the July 22, 1992 jet

Component	T_{SXT} ($\times 10^6$ K)	EM_{SXT} ($\times 10^{45}$ cm^{-3})	17 GHz Flux (predicted; SFU)	17 GHz Flux (Observed; SFU)
Source A	4.7 ± 1.3	6 ± 1.7	0.0065 ± 0.0025	0.16
Source B	4.55 ± 0.65	8 ± 1.5	0.008 ± 0.002	0.18
Source C	5.45 ± 1.35	310 ± 60	0.285 ± 0.025	0.23

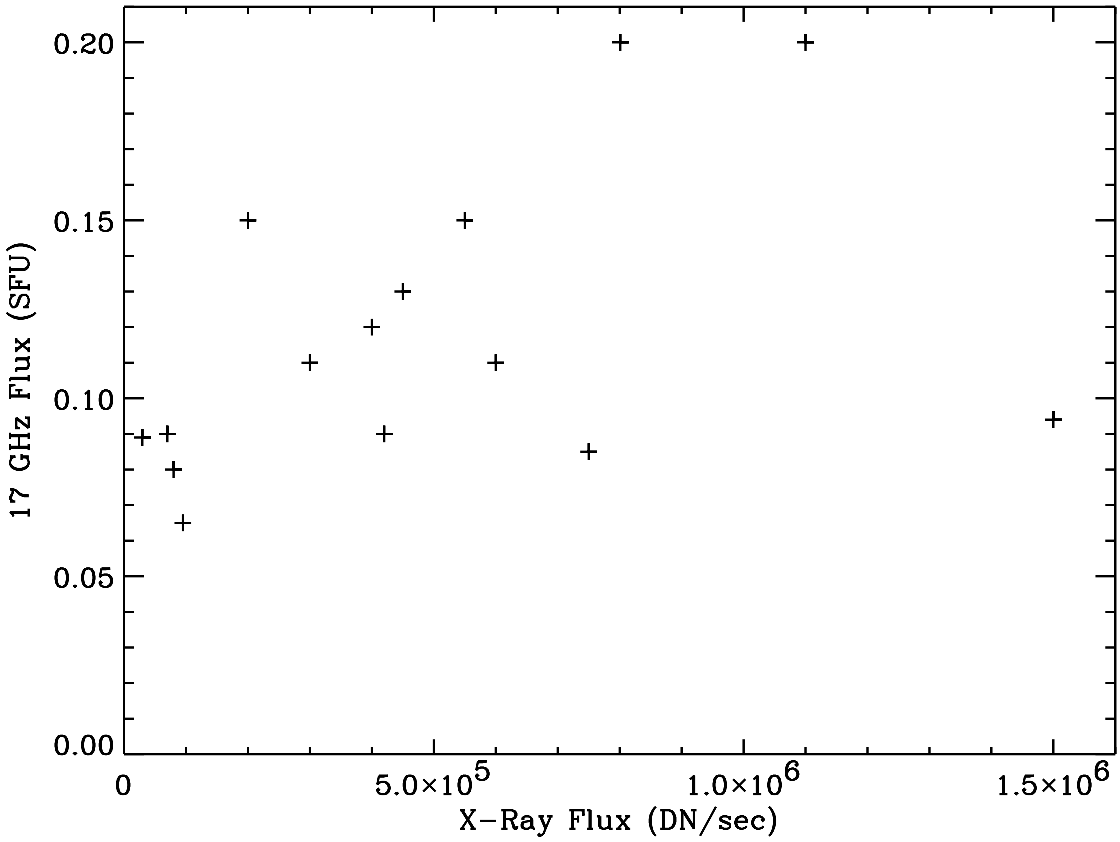
0.20
0.15
0.10
0.05
0.00
17 GHz Flux (SFU)
0
5.0×10^5
1.0×10^6
1.5×10^6
X-Ray Flux (DN/sec)

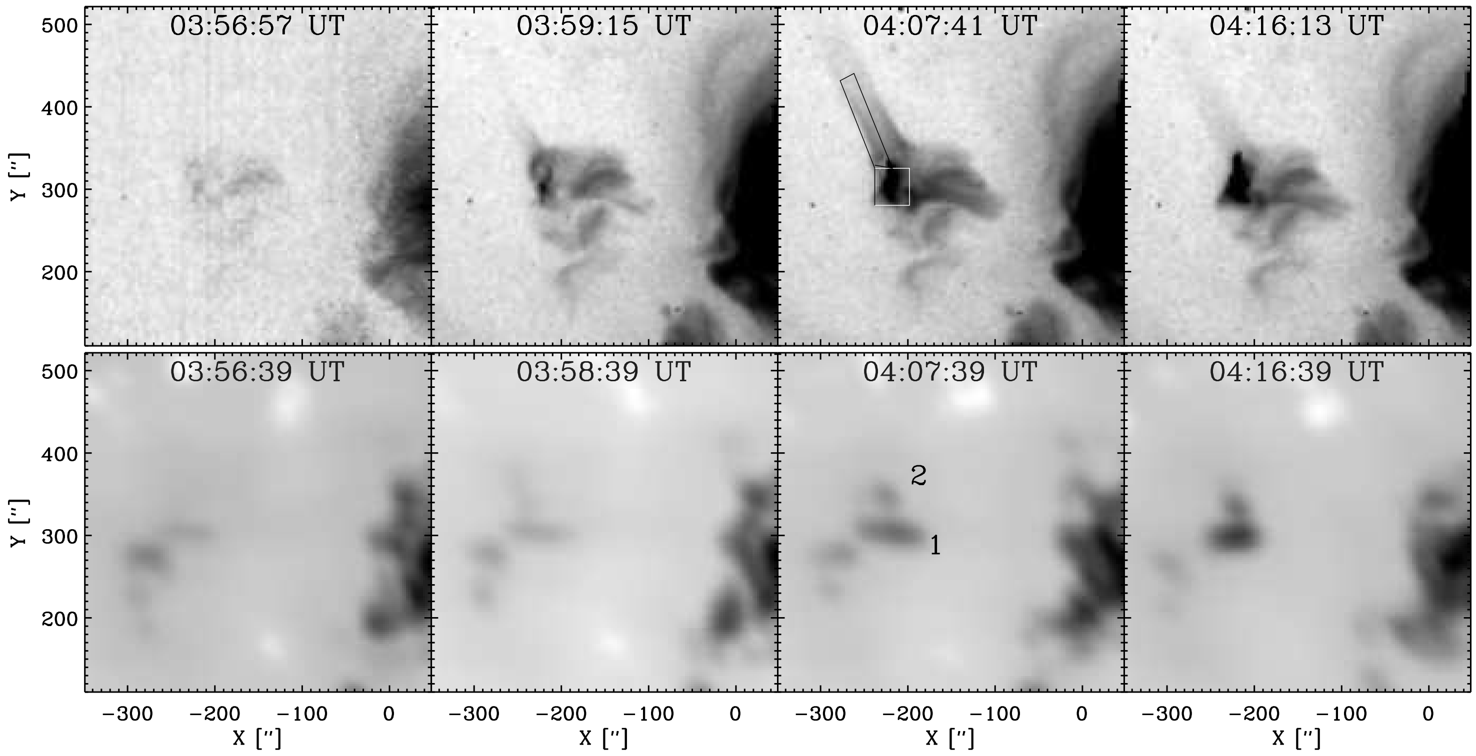
03:56:57 UT
03:59:15 UT
04:07:41 UT
04:16:13 UT
03:56:39 UT
03:58:39 UT
04:07:39 UT
04:16:39 UT
1
2
Y ["]
X ["]
500
400
300
200
−300
−200
−100
0

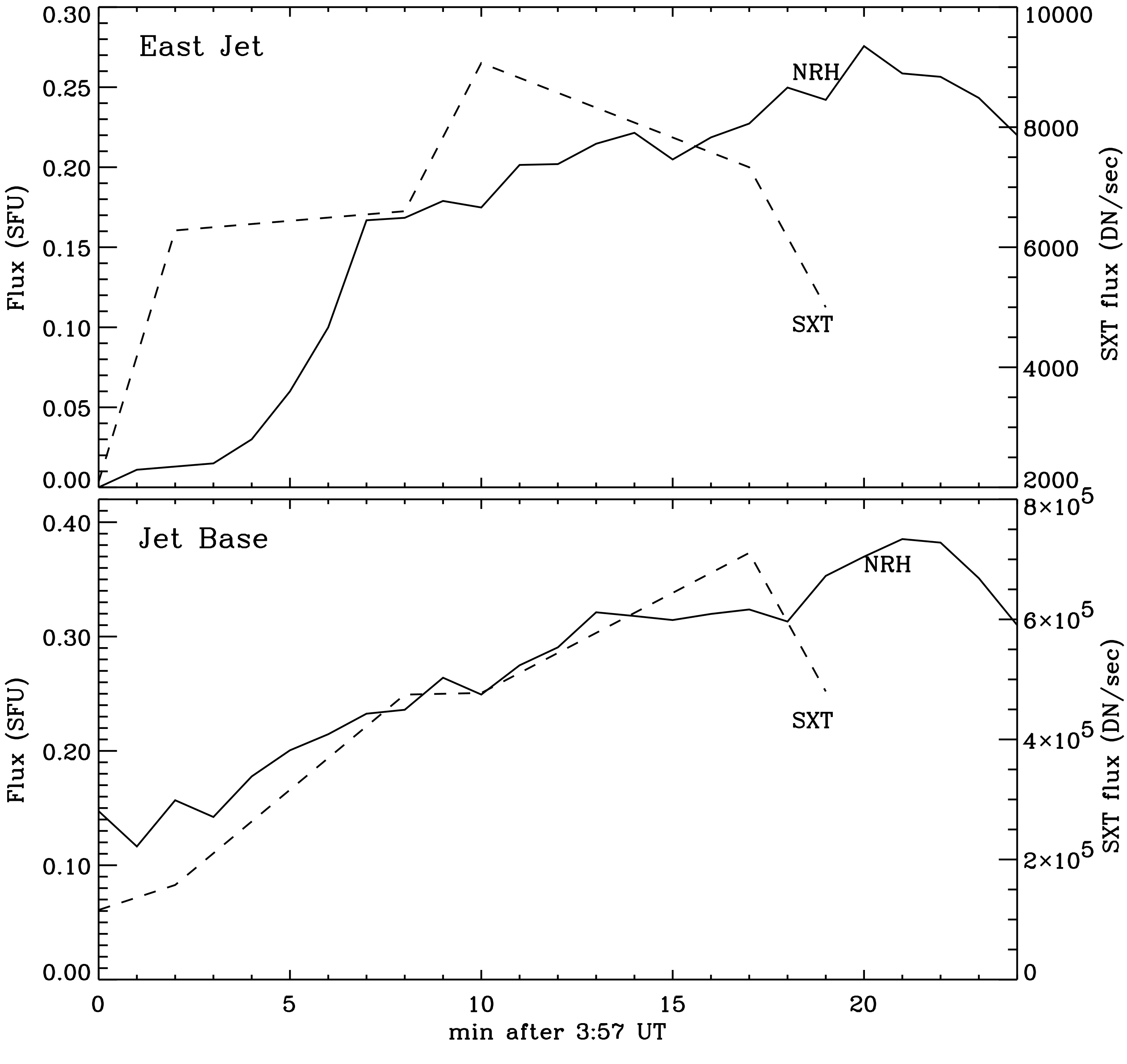

East Jet
NRH
SXT
Flux (SFU)
SXT flux (DN/sec)
0.00
0.05
0.10
0.15
0.20
0.25
0.30
2000
4000
6000
8000
10000
Jet Base
NRH
SXT
Flux (SFU)
SXT flux (DN/sec)
0.00
0.10
0.20
0.30
0.40
0
2×10^5
4×10^5
6×10^5
8×10^5
0
5
10
15
20
min after 3:57 UT

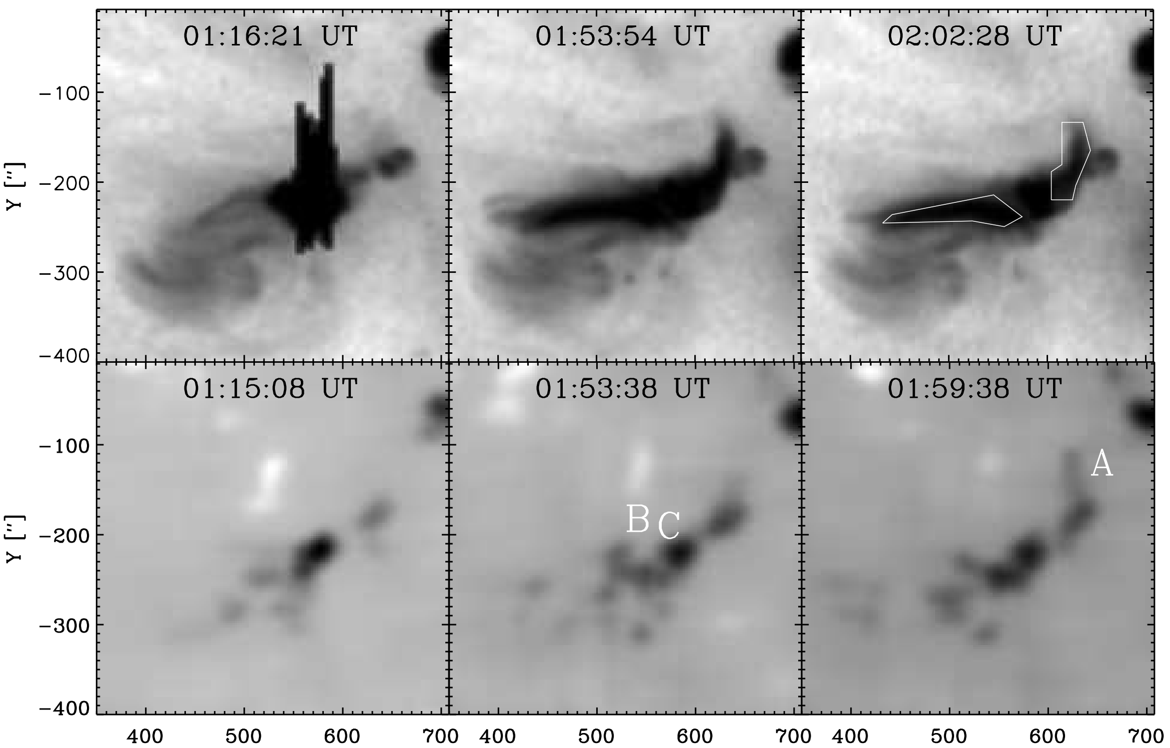
01:16:21 UT
01:53:54 UT
02:02:28 UT
01:15:08 UT
01:53:38 UT
01:59:38 UT
A
B
C
Y ['']
X ['']
−100
−200
−300
−400
400
500
600
700

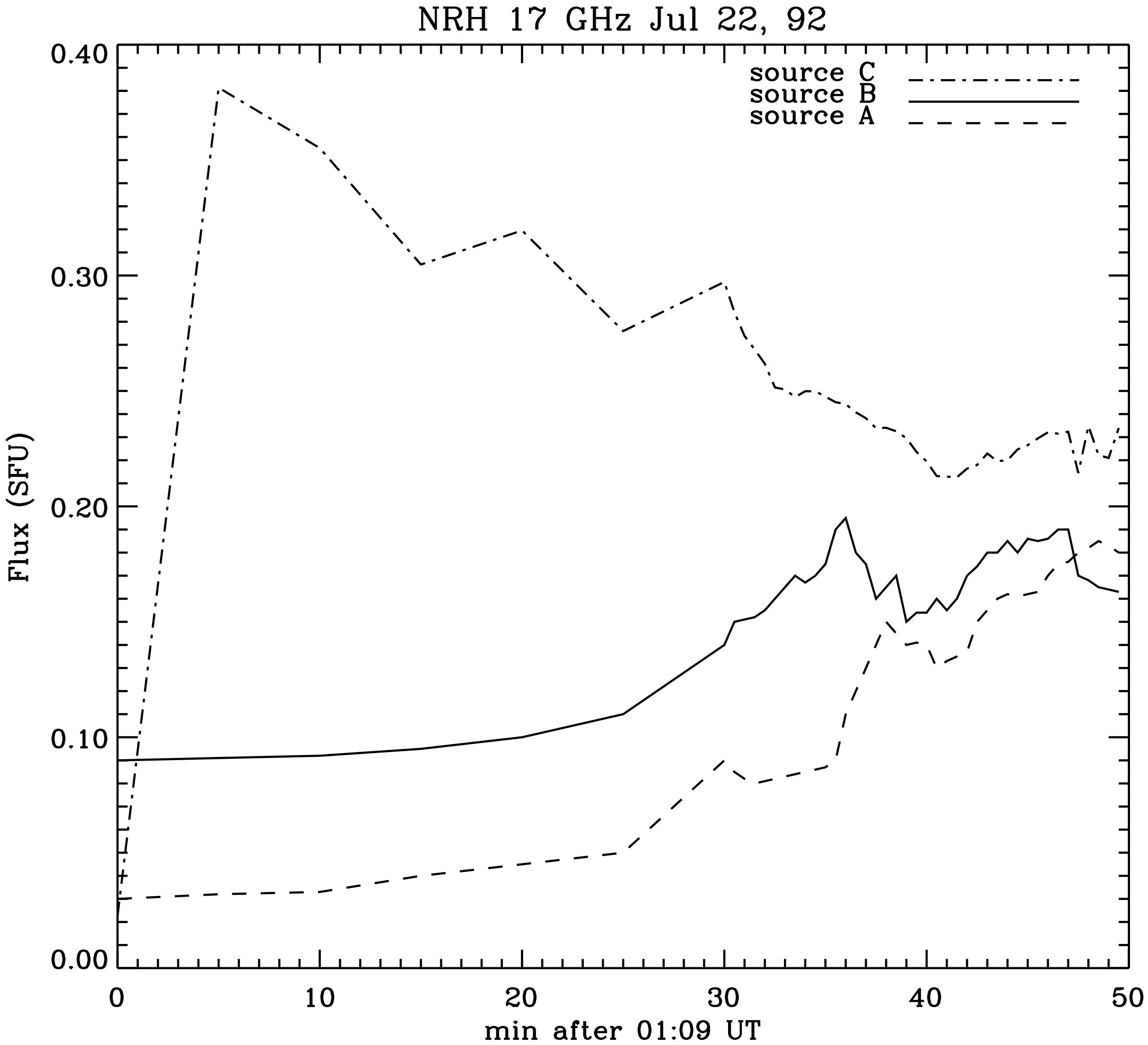
NRH 17 GHz Jul 22, 92
source C
source B
source A
Flux (SFU)
0.00
0.10
0.20
0.30
0.40
0
10
20
30
40
50
min after 01:09 UT